Processing of Porous Hydroxyapatite Scaffold

A THESIS SUBMITTED IN PARTIAL FULFILMENT
OF THE REQUIREMENT FOR THE DEGREE OF

Master of Technology
in
Ceramic Engineering

By

Sanjaya Kumar Swain

Department of Ceramic Engineering
National Institute of Technology
Rourkela
2009

Processing of Porous Hydroxyapatite Scaffold

A THESIS SUBMITTED IN PARTIAL FULFILMENT
OF THE REQUIREMENT FOR THE DEGREE OF

Master of Technology

In

Ceramic Engineering

By

Sanjaya Kumar Swain

Under the guidance of

Dr. S. Bhattacharyya

Department of Ceramic Engineering

National Institute of Technology

Rourkela

2009

CERTIFICATE

This is to certify that the thesis entitled, “Processing of Porous Hydroxyapatite Scaffold” submitted by Mr. Sanjaya Kumar Swain in partial fulfillment of the requirement for the award of Master of Technology Degree in Ceramic Engineering at the National Institute of Technology, Rourkela (Deemed University) is an authentic work carried out by him under my supervision and guidance.

To the best of my knowledge, the matter embodied in the thesis has not been submitted in any other University/Institute for the award of any Degree or Diploma.

Date:

Prof. S.BHATTACHARYYA
Dept. of Ceramic Engineering
National Institute of Technology
Rourkela-769008

ACKNOWLEDGEMENT

I wish to express my deep sense of gratitude and indebtedness to **Prof. S.Bhattacharyya,** Department of Ceramic Engineering, N.I.T Rourkela for assigning me the project “Processing of Porous Hydroxyapatite Scaffold” and for his inspiring guidance, constructive criticism and valuable suggestion throughout this project work.

I would like to express my gratitude to **Prof. S. K. Pratihar, Prof. J. Bera, Prof. B.B.Nayak, Prof. S.Pal, and Prof. R.Mazumdar** for their valuable suggestions and encouragements at various stages of the work.

I am also thankful to **Mr. Yuogojoti Nayak** and other research scholars in Department of Ceramic Engineering for providing all joyful environments in the lab and helping me throughout this project.

Last but not least, my sincere thanks to all my friends who have patiently extended all sorts of help for accomplishing this undertaking.

Sanjaya Kumar Swain
M.Tech
Ceramic Engineering

ABSTRACT

Hydroxyapatite ceramics have been recognized as substitute materials for bone and teeth in orthopaedic and dentistry field due to their chemical and biological similarity to human hard tissue. It is biocompatible and bioactive material that can be used to restore damaged human calcified tissue. Porous hydroxyapatite exhibits strong bonding to the bone, the pores provide a mechanical interlock leading to a firm fixation of the material. Porous hydroxyapatite is more resorbable and more osteoconductive than its dense counterpart and in porous form the surface area is greatly increased which allows more cells to be carried in comparison with dense hydroxyapatite. The HA prepared from $CaNO_3 4H_2O$ and $(NH_4)_2HPO_4$ by co-precipitation method was phase pure at temperature 1250^0C. Porous scaffold was prepared by polymeric sponge and incorporation of fugitive such as naphthalene and PEG. Porous HA prepared from polymeric sponge method had about 70% porosity having pore diameter~400-500µm and pores were interconnected. With increase in PVA contents from 2 to 5 wt% with 40% solid loading the strength of the scaffold increased from 0.69-1.02MPa. It was studied that porosity, pore size and pore inter connectivity depends upon the slurry concentration and the amount of pore former used. In HA-PEG scaffold the porosity increased with PEG 4000 content, while it is decreased for PEG 6000 and pore size depends upon the molecular weight of PEG. In HA-naphthalene scaffold the porosity increased with increased the amount of pore former. It was observed that range of porosity~1-100µm obtained by varying the amount and size of ceramic and PEG particles. The molecular weight of PEG plays an important role in the morphology, structure, and pore size of scaffold. In-vitro bioactivity and biodegradability studies show that the synthesized scaffold from various methods was bioactive as well as bioresorbable.

CONTENTS

Chapter-1

Introduction

Introduction:

A key component in tissue engineering for bone regeneration is the scaffold that serves as a template for cell interactions and the formation of bone-extracellular matrix to provide structural support to the newly formed tissue [1]. Scaffolds for bone regeneration should meet certain criteria to serve this function, including mechanical properties similar to those of the bone repair site, biocompatibility and biodegradability at a rate commensurate with remodeling. Scaffolds serve primarily as osteoconductive moieties, since new bone is deposited by creeping substitution from adjacent living bone. Scaffolds for osteogenesis should mimic bone morphology, structure and function in order to optimize integration into surrounding tissue [1]. Bone is a structure composed of hydroxyapatite ($Ca_{10}(PO_4)_6(OH)_2$) crystals deposited within an organic matrix. The morphology is composed of trabecular bone which creates a porous environment with 50–90% porosity. Four cell types are present in bone tissue: osteoblasts, osteoclasts, osteocytes and bone lining cells. Bone is at a constant state of remodeling with osteoblasts producing and mineralizing new bone matrix, osteocytes maintaining the matrix and ostoclasts resorbing the matrix. Bone lining cells are inactive cells that are believed to be precursors for osteoblasts [2]. Scaffold properties depend primarily on the nature of the biomaterial and the fabrication process. The nature of the biomaterial has been the subject of extensive studies including different materials such as metals, ceramics, glass, chemically synthesized polymers, natural polymers and combinations of these materials to form composites.

Porosity is defined as the percentage of void space in a solid and it is a morphological property independent of the material [3]. Pores are necessary for bone tissue formation because they allow migration and proliferation of osteoblasts and mesenchymal cells, as well as vascularization [4]. In addition, a porous surface improves mechanical interlocking between the implant biomaterial and the surrounding natural bone, providing greater mechanical stability at this critical interface. The most common techniques used to create porosity in a biomaterial are salt leaching, gas foaming, phase separation, freeze-drying and sintering depending on the material used to fabricate the scaffold. The minimum pore size required to regenerate mineralized bone is generally considered to be ~100 μm [5].

1.1. Hydroxyapatite (HA):

Hydroxyapatite [$Ca_{10}(PO_4)_6(OH)_2$] is one of the most biocompatible ceramics because of its significant chemical and physical resemblance to the mineral constituents of human bones and teeth. It is a bioactive ceramics widely used as powders or in particulate forms in various bone repairs and as coatings for metallic prostheses to improve their biological properties. It has excellent biocompatibility, bioactivity and osteoconduction properties. HA is thermodynamically the most stable calcium phosphate ceramic compound nearest to the pH, temperature and composition of the physiological fluid. Recently, HA has been used for a variety of biomedical applications,

including matrices for drug release control. Due to the chemical similarity between HA and mineralized bone of human tissue, synthetic HA exhibits strong affinity to host hard tissues. Formation of chemical bond with the host tissue offers HA a greater advantage in clinical applications over most other bone substitutes, such as allograft or metallic implants. HA possesses a hexagonal structure with a P63/m space group and cell dimensions a=b=9.42 Å, and c=6.88 Å, whereP63/m refers to a space group with a six-fold symmetry axis with a three-fold helix and a micro plane. It has an exact stoichiometric Ca/P ratio of 1.67 and is chemically very similar to the mineralized human bone. However, despite chemical similarities, mechanical performance of synthetic HA is very poor compared to bone. In addition, the bone mineral present a higher bioactivity compared to synthetic HA [5].

Many researchers have observed that the mechanical strength and fracture toughness of HA ceramics can be improved by the use of different sintering techniques which include addition of a low melting secondary phase to achieve liquid phase sintering for better densification, incorporation of sintering additives to enhance densification through grain boundary strengthening, and use of nano scale ceramic powders for better densification contributed by large surface area to volume ratios of nano-size powders.

The preparation of HA bioceramic materials have been carried out using different approaches like sol–gel, hydrothermal processing, microwave route, precipitation route, emulsion system and sonochemical synthesis.

1.2. Porous Hydroxyapatite:

Porous HA exhibits strong bonding to the bone; the pores provide a mechanical interlock leading to a firm fixation of the material. Bone tissue grows well into the pores, thus increasing strength of the HA implant. The ideal bone substitute is a material that will form a secure bond with the tissues by allowing, and even encouraging, new cells to grow and penetrate. One way to achieve this is to use a material that is osteophilic and porous, so that new tissue, and ultimately new bone, can be induced to grow into the pores and help to prevent loosening and movement of the implant. A porous hydroxyapatite coating facilitates bone growth through a highly convoluted interface. When pore sizes exceed 100 μm, bone grows through the channels of interconnected surface pores, thus maintaining the bone's vascularity and viability [4]. Since porous HA is more resorbable and more osteoconductive than dense HA, there is an increasing interest in the development of synthetic porous hydroxyapatite (HA) bone replacement materials for the filling of both load-bearing and non-load-bearing osseous defects. Simulating the human bone structure, porous HA scaffold has large surface area, which is beneficial for adhesion of biological tissue cell and growth of new bone phase [4].

Porous HA implants have served as bone substitute in the clinics since long. HA with controlled porosity is analogous to the natural ceramic in the bone and is bioactive in the sense that

it is a non-toxic compound and interfacial bonds are able to develop between HA and the living tissues leading to enhanced mechanical strength of the overall structure. The porosity aids in tissue growth and their binding with the HA. However, lower mechanical strength of pure HA has hampered its use as a bone implant material because of conflicting requirements of porosity and strength.

1.3. Methods available to make porous hydroxyapatite

Process	Description /Comments
Replamineform process	Replication of an echinoid skeletal macrostructure or coral (White et al) [6]
Direct conversion of natural Coral to HAP	Occurs via hydrothermal reaction (Ray et al)[7]
Changing natural cancellous bone to ceramic	Hing et al. [8]
Slurry foaming method	Foaming agent -hydrogen peroxide (H_2O_2) (Ryshkewith et al.) [9] carbonate salt and acid (Westerduin)
Solid state reaction	Calcium carbonate and dicalcium phosphate forming Hap, H_2O and CO_2 (Arita et al.) [10]
Dry –state compression of HA powder with pore maker.	Pore maker - wax, polymer beads, or fugitive phase materials which are burned off [11]
Starch consolidation	Mixing Starch suspension with dry Hap powder under stirring and the burning of the Starch (Rodriguez et al.) [12]
Negative replica method	A polymer bead network is used to create a Negative replica of HA (Richart et al.) [13] or Cellulose sponge imbibitions is used (Martinetti et al.) [14]
Positive replica method	A polymeric sponge method is used (slip casting), or a reticulate polymeric foam is used to create a positive replica of HAP (Woyansky et al.) [15]
Negative–negative replica method	Cancellous bone is used to create a negative replica, afterwards acid is used to remove the bone and a Hap Negative replica of wax mold is formed (Tancred et al.) [16]
Combination of gel casting and foaming	Sepulvenda et al. [17]

1.4. Necessity for porous hydroxyapatite:

The necessity for porosity in bone regeneration has been shown by Kuboki et al. [18] using a rat

ectopic model and solid and porous particles of hydroxyapatite for BMP-2(bone morphogenic proteins) delivery; no new bone formed on the solid particles, while in the porous scaffolds direct osteogenesis occurred. Further support comes from studies with metal porous-coated implants compared to the non coated material. Treatment of titanium alloy implant surfaces with sintered titanium beads created a porous coating that enhanced cortical shear strength of the implants recovered from sheep tibiae, while further coating with beads with hydroxyapatite did not result in significant improvement. Titanium fiber-metal porous coatings (45% porosity and 350μm average pore size) maximized bone in growth and increased the potential for stress-related bone resorption of femoral stems in a canine total hip arthroplasty model [19]. A similar result was observed for plasma spray-coated titanium implants with 56–60% porosity, although bone in growth was maximized for an open-pore titanium fiber mesh (60% porosity and 170 μm average pore size) coated with polyvinyl alcohol hydrogel [20].

D'Lima et al. [21] showed that surface roughness was more important for osseointegration of titanium implants in rabbit femurs, since an acid-etched coating (highest surface roughness) showed a higher overall osseointegration when compared with grit-blasted and fiber mesh (average pore size 400 μm) coatings. The presence of a thicker (600–1000 nm) porous(13–24% porosity, pores less than 8 μm) oxide film on the surface of titanium screws resulted in more bone formation when implanted in tibia defects in rabbits compared to controls with a nonporous oxide layer of 17–200 nm in thickness. Lower porosity of the oxide layer (19% versus 24%) resulted in decreased surface roughness (0.97 versus 1.02 mm) as measured by confocal laser scanning profilometry. Coating titanium alloy implants with a 50 μm layer of porous hydroxyapatite did not increase the percentage of osseointegrated surface in the mandible of dogs, although bone extended into the micropores of hydroxyapatite resulting in an osseous micro-interlocking [22]. However, in the maxillae there was more bone opposing the coated implants suggesting a beneficial effect for areas of poorer bone quality [22]. Although macro porosity (pore size 450 μm) has a strong impact on osteogenic outcomes, micro porosity (pore size 10 μm) and pore wall roughness play an important role as well; hydroxyapatite ceramic rods with average pore size of 200 μm and smooth and dense pore walls failed to induce ectopic bone formation in dogs, in contrast to rods made from the same material with average pore size 400 μm but with rough and porous pore walls.

Micro porosity results in larger surface area that is believed to contribute to higher bone inducing protein adsorption as well as to ion exchange and bone-like apatite formation by dissolution and re-precipitation. Surface roughness enhances attachment, proliferation and differentiation of anchorage dependent bone forming cells. The solid free form fabrication technique allowed the fabrication of poly(desaminotyrosyl-tyrosine ethyl ester carbonate) (a tyrosine derived pseudo-polyamino acid) scaffolds with four axial and four radial channels and fixed 500 μm pores separated by 500 μm solid walls or 80% porous walls. Scaffolds from the same material with random pore distributions served as controls. Although there was no statistical difference in the

bone formed in cranial defects in rabbits, bone in growth followed the architecture of the scaffolds; a continuous in growth from the outer periphery was observed in the random pore size scaffolds, while scaffolds with same sized pores and solid walls promoted discontinuous in growth with bone islands throughout the whole scaffold; scaffolds with same sized pores and porous walls resulted in both types of bone ingrowths. It was hypothesized that discontinuous bone in growth may result in faster healing, since bone will be forming not only from the margins but also throughout the whole space of the defect [23]. These studies demonstrate the enhanced osteogenesis of porous versus solid implants, both at the macroscopic as well as the microscopic level.

1.5. Requirements for ceramic –bone tissue engineering scaffold

Property	factors
Material property	Chemical composition (purity, crystallinity) powder processing route (commercial or lab made), raw-powder particle size and its distribution, Sintering parameter (temperature and time) mechanical properties.
Porous structure property	Pore size and distribution, pore shape, porosity Interconnection, microporosity (bulk or surface), specific surface area.
Tissue interaction	Bio-compatibility, resorption rate and degradation behavior.
Geometric property	sample size, volume, and weight;

1.6. Application of porous HA:

Porous HA have been applied for cell loading, drug releasing agents, chromatography analysis, and the most extensively for hard tissue scaffolds. Various cell products are therapeutically of crucial significance including hormones, enzymes, vaccines, and nucleic acids which could improve the technology of the diagnosis and treatment of human diseases. Mammalian cells can be grown and maintained in-vitro, but are generally anchorage-dependent, i.e., they need solid substrate for growth [24].

Microcarrier culture technique is one of the methods developed for cell cultivation. Owing to high surface area for cells to adhere and grow, microcarrier culture offers a practical high yield culture of anchorage-dependent cells and thus it is possibly suitable for large-scale operations. A variety of microcarriers, including those based on dextran, polystyrene or cellulose, and collagen or

gelatin based macroporous beads have been developed. The mean diameter of microcarriers often lies in the range 130–200 μm, even though a range as wide as 100–400 μm has been described as suitable for growth.

In drug delivery systems, it has been recognized that a system for the slow, local and continuous release of drugs would be a decided advantage for the treatment of many ailments. One of the potential candidates for such controlled drug delivery systems is porous ceramics; much attention has been paid to porous HA. For example, chronic disease or localized surgical intervention, relying on a sustained local drug delivery needs ceramic capsule suitable to release drugs at a controlled rate. Bone drug delivery systems were also developed using porous calcium phosphate ceramics bonded with antibiotics through a biodegradable polymeric matrices. Porous HA has been extensively applied for artificial bone substitutes. The primary purpose of tissue engineering is repair, regeneration, and reconstruction of lost, damaged or degenerative tissues [25].

Objective of present study:

- Synthesis of HA by co-precipitation method by using Ca $(NO_3)24H_2O$ and $(NH_4)_2HPO_4$.
- Processing of porous HA scaffolds by polymeric sponge method and using pore former PEG and naphthalene.
- Study of porosity, bulk density, compressive strength, pore size, pore size distribution and microstructure of porous HA scaffolds by varying solid loading, binder contents, amount and size of pore former.
- In-vitro study of bioactivity and biodegradability of porous HA scaffolds.

Chapter-2

Literature Review

Literature Review:

Soon-Ho kwon et al. [26] successfully fabricated porous bioceramics with variable porosity, using the poly urethane sponge technique. Porosity was controlled by the number of coatings on the sponge struts. When a porous body was produced by a single coating, the porosity was ~90%, and the pores were completely interconnected. When the sintered body was coated five times after the porous network had been made, the porosity decreased to 65%. The compressive strength was strongly dependent on the porosity and weakly dependent on the type of ceramics, HA, TCP, or HA/TCP composite. At the 65% porosity level, the strength was ~3MPa. The TCP exhibited the highest dissolution rate in a Ringer's solution, HA had lowest rate. The biphasic HA/TCP showed an intermediate dissolution rate. The biodegradation of calcium phosphate ceramics could be controlled by simply adjusting the amount of HA or TCP in the ceramic.

Shi Hong Li et al. [27] studied novel method to manufacture porous hydroxyapatite by dual phase mixing. The technique is based on mixing to immiscible phases HA slurry and polymehtylmethacrylate (PMMA) resin. Naphthalene particles are necessary when grater porosity (>50%) is wanted. The majority of pores could be located within the range of 200-300 μm for HA with 50% porosity. The average compressive strength was 8.9MPa for 50% porous HA and was only 4.8MPa for the HA with 60% porosity. By controlling the process parameters such as the viscosity of HA slurry, the hydroxyapatite/polymethylmethacrylate (HA/PMMA) ratio, or the mixing time and speed, it is possible to adjust porosity, pore size, and interconnectivity.

Schwartzwalder and Somers [28] studied the slurry infiltration process for making porous ceramics. In this process poly urethane (PU) foam was infiltrated with ceramic slurry and the body was compressed by passing it through a set of rollers to remove the excess slurry. In this manner the slurry remained coated on the PU struts and open pore channels were left in between. The coated PU perform was then dried, followed by burn out of the PU and sintering at higher temperature. The foams produced were reticulated foams with porosity within the range 75-90%. Zhu et al. [29] investigated the influence of the compressive strain during roll pressing and the number of passes on the foam microstructure. It was seen that the quality of slurry coating on to PU struts was strongly dependent on the magnitude of compressive strain than the number of passes. Higher compressive strain resulted in thinner slurry coating on the struts and lower bulk density. The coating of slurry onto PU struts was also affected by slurry viscosity. Highly fluid slurries were not very effective in coating the PU foam struts resulting in accumulation of slurry at the bottom of PU foam. Pu et al. [30] pointed that the conventional roll pressing procedure results in accumulation of slurries at the joint of the polymeric struts.

K. lin et al. [31].studied on the preparation of macroporous calcium silicate ceramics by using PEG as pore former. Sintered compact with porosity in the range of 40-75% have been obtained by varying the amount and size of ceramic and PEG particles and the sintering temperature. Molecular weight of PEG plays an important role in the morphology, structure and the pore size of the

microporous calcium silicate. The PEG plays a main role in larger pore formation, when enough mass of PEG with lower molecular weight were added. The available contents of PEG additive in the mixture solution have to decrease in the case of larger molecular weight of PEG than that of smaller molecular weight of PEG according to the degree of miscibility.

Nursen Koc et al. [32] studied the fabrication and characterization of porous tricalcium ceramics by using a modified slip casting technique. The slip was prepared by suspending custom-made TCP powder and PMMA beads in an aqueous medium stabilized with an acrylic deflocculant. Porous TCP ceramics were obtained by sintering the polymer-free preforms for 2 h at 1000^0C. The ceramic was prepared from a casting slip which contained 70% polymer beads in the size range 210–250 μm. The average size of large pores in the sintered ceramic was around 190 μm. Higher proportions of polymer beads in slip solids led to the development of highly porous ceramics with thinner walls. As the amount of polymer beads was raised, the size of interconnections increased proportionately. A porosity network of this nature would allow free circulation of body fluids.

Han Guo et al. [33] studied biocompatibility and osteogenicity of degradable Ca-deficient hydroxyapatite scaffolds from calcium phosphate cement for bone tissue engineering by a particle leaching method. The morphology, porosity and mechanical strength as well as degradation of the scaffolds were characterized. The results indicated that the CDHA scaffolds with a porosity of 81% showed open macropores with pore sizes of 400–500 μm. Thirty-six per cent of these CDHA scaffolds were degraded after 12 weeks in Tris–HCl solution. The results revealed that the CDHA scaffolds were biocompatible and had no negative effects on the mesenchymal stem cells (MSCs) in-vitro. The in-vivo biocompatibility and osteogenicity of the scaffolds were investigated. The CDHA scaffold after 8 week implantation shows good biocompatibility and extensive osteoconductivity.

YueJun Tang et al. [34] studied on the preparation of uniform porous hydroxyapatite biomaterials by a new method. Uniform porous biomaterials in the form of disk samples were prepared by the mixture of hydroxyapatite (HAP) powders and monodispersed polystyrene microspheres, and then HAP uniform porous materials with different diameter and different porosity (diameter: 436 ± 25 nm, 892 ± 20 nm and1890 ± 20 nm, porosity: 46.5%, 41.3% and 34.7%, respectively) were prepared by sintering these disk samples at 1250^0C for 5 h.

Marek Potoczek [35] studied the gel casting of hydroxyapatite foams using agarose as gelling agent and the rheological behavior of the suspensions. The viscosity of the slurries could be adjusted by agarose concentration and HA solid loading. These parameters were essential in tailoring the porosity as well as the cell and window sizes of the resulted HA foams. Depending of HA solid loading (24–29 vol.%) and agarose concentration (1.1–1.5 wt.% with regard to water) in the starting slurry, the mean cell size ranged from 130 to 380 μm, while the mean window size varied from 37 to 104 μm. Depending on the porosity range (73–92%) and related with this parameter the mean cell and window size, the compressive strength of HA foams was found to be in the range 0.8–5.9 MPa.

Hyun-Min Kim et al. [36] studied the Process and kinetics of bonelike apatite formation on sintered

hydroxyapatite in a simulated body fluid. The surfaces of two hydroxyapatites (HA), which have been sintered at different temperatures of 800 and 1200 ^{0}C, was investigated as a function of soaking time in simulated body fluid (SBF) using transmission electron microscopy (TEM) attached with energy-dispersive spectrometry (EDX) and laser electrophoresis spectroscopy. The HAs reveal negative surface charge and thereby interact with the positive calcium ions in the fluid to form the Ca-rich ACP, which gains positive surface charge. The Ca-rich amorphous calcium phosphate (ACP) on the HAs then interacts with the negative phosphate ions in the fluid to form the Ca-poor ACP, which stabilizes by being crystallized into bonelike apatite. This process of apatite formation was shown to be sluggish on the HA sintered at higher temperature. This phenomenon is attributed to initial lower negative surface charge of the HA sintered at higher temperature owing to a poverty in surface hydroxyl and phosphate groups, which are responsible for the surface negativity. The process and kinetics of apatite formation on HA could be affected by bulk factors such as density and surface area as well as by surface factors such as composition and structure. The iso-electric point of HA in water is at pH ranging between 5 and 7, and is lower than the pH of the SBF (7.4). Therefore on immersion in SBF, the HA could reveal negative surface charge by exposing hydroxyl and phosphate units in its crystal structure. The HA surface uses this negative charge to interact specifically with the positive calcium ions in the fluid, consequently forming a Ca-rich ACP. The formation of the Ca-rich ACP is assumed to take place in consecutive accumulation of the calcium ions, which makes the Ca-rich ACP acquire and increase positive charge. The Ca-rich ACP on the HA therefore interacts specifically with the negative phosphate ions in the fluid to form a Ca-poor ACP. This type of Ca-poor ACP has been observed as a precursor, which eventually crystallizes into bonelike apatite on various bioactive ceramics.

A.Cuneyt Tas [37] studied the synthesis of biomimetic Ca-hydroxyapatite powders at 37^{0}C in synthetic body fluids. Hydroxyapatite (HA, $Ca_{10}(PO_4)_6(OH)_2$), was prepared as a nano-sized (~50 nm), homogeneous and high-purity ceramic powder from calcium nitrate tetrahydrate and diammonium hydrogen phosphate salts dissolved in modified synthetic body fluid (SBF) solutions at 37^{0}C and pH of 7.4 using a novel chemical precipitation technique. The synthesized precursors were found to reach a phase purity of 99% easily after 6h of calcination in air atmosphere at 900^{0}C, following oven drying at 80^{0}C. When appropriate amounts of $Ca(NO_3)_2$ $4H_2O$ were dissolved in SBF, a slight turbidity was observed in the beakers due to the immediate formation of fine precipitates, viz. “seeds”. The seeds were found to be amorphous (by XRD) in their as-recovered forms. Heating of the precursor seeds in air atmosphere at the temperature range of 900-1170^{0}C caused them to crystallize.

Deville et al. [38] studied the freeze casting of porous hydroxyapatite scaffolds and observed that by varying the freezing rate of slurry as well as slurry concentration, porosities in the range 40-60% could be achieved. The pores were open and unidirectional and exhibited a lamellar morphology. The processed scaffolds exhibited high compressive strength up to 145 MPa.

Itatani K et al. [39] studied the preparation of Porous Hydroxyapatite Ceramics from Hollow Spherical Agglomerates Using a Foaming Agent of H_2O_2 and observed that by changing the concentration of H_2O_2 solution from 0 to 20mass%, the total porosity of HA compact fired at 1000^0C for 5h could be changed linearly from 61.2 to 71.7%. The HA compact exhibited pore sizes with maximum porosity (71.7%) at around 0.7 μm, 5-100 μm and 100-200 μm.

Lyckfeldt and Ferreira [40] demonstrated the use of potato starch as both consolidator/binder and pore former in forming porous ceramics. In this process, 16-60% starch was added as dry power weight basis to ceramic slips and homogenized 2h. The above homogenized slip was consolidated in a mould at 80^0c, followed by drying, binder burn out and sintering of bodies. Pore sizes in the range 10-80 μm and porosity between 23 and 70% was obtained by varying ceramic loading, the nature and amount of starch incorporated in the compacts. Increasing the amount of a certain type of starch resulted in large pore size due to greater degree of contact among the starch particles.

Thijs et al. [41] studied a novel technique to produce macroporous ceramics using seeds and peas as sacrificial core materials. The first step in this technique was to coat the seeds, peas with wetting ceramic slurry that undergoes gelation. The coated seeds and peas were consolidated by packing them in a container and infiltrating with ceramic slurry which underwent gelation. The compacts thus obtained were subjected to the conventional steps of drying, binder burn out and sintering. The resulting bodies had greater than 90% porosity with pore size determined by the size of the seeds, peas.

Mehdi Kazemzadeh Narbat et al. [42] studied on fabrication of porous hydroxyapatite-gelatin composite scaffolds for bone tissue engineering. It was observed that the prepared scaffold has an open, interconnected porous structure with a pore size of 80-400μm, which is suitable for osteoblast cell proliferation. The mechanical properties of different weight fraction of HA (30, 40, and 50 wt%) was assessed and it was found that the GEL/HA with ratio of 50wt% HA has the compressive modulus of ~10 Giga Pascal (GPa), the ultimate compressive stress of ~32 Mega Pascal (MPa) and the elongation of ~3MPa similar to that of trabecular bone. The porosity and the apparent density of 50wt% HA scaffold were calculated and it was found that the addition of HA content can reduce the water absorption and the porosity.

Xiao Huang et al. [43] studied the HA-based composite scaffolds that have a unique macroporous structure and special struts of a polymer/ceramic interpenetrating composite. A novel combination of polyurethane (PU) foam method and a hydrogen peroxide (H_2O_2) foaming method is used to fabricate the macroporous HA scaffolds. Micropores are present in the resulting porous HA ceramics after the unusual sintering of a common calcium phosphate cement and are infiltrated with the poly(D,L-lactic-co-glycolic acid) (PLGA) polymer. The internal surfaces of the macropores are further coated with a PLGA bioactive glass composite. It is found that the HA scaffolds fabricated by the combined method show high porosities of 61–65% and proper macropore sizes of 200–600 μm.

The PLGA infiltration improved the compressive strengths of the scaffolds from 1.5–1.8 to 4.0–5.8MPa.

Vassilis Karageorgiou and DavidKaplan [44] studied the porosity of 3D biomaterial scaffolds and osteogenesis. It has been seen that porosity and pore size of biomaterial scaffolds play a critical role in bone formation in-vitro and in-vivo. This review explores the state of knowledge regarding the relationship between porosity and pore size of biomaterials used for bone regeneration. The effect of these morphological features on osteogenesis in-vitro and in-vivo, as well as relationships to mechanical properties of the scaffolds, is addressed. In-vitro, lower porosity stimulates osteogenesis by suppressing cell proliferation and forcing cell aggregation. In contrast, in-vivo, higher porosity and pore size result in greater bone ingrowth. The minimum requirement for pore size is considered to be~100 μm due to cell size, migration requirements and transport. However, pore sizes ~300 μm are recommended, due to enhanced new bone formation and the formation of capillaries.

I. Sopyan et al. [45] studied on Porous hydroxyapatite for artificial bone applications. It was reported that the preparation of HA porous bodies via polymeric sponge method; the samples which were prepared using sol–gel method-derived HA powders and commercial HA powders showed a considerable compressive strength ranging from 1.3 to 10.5MPa for the increased apparent density from 1.27 to 2.01 g/cm^3. This is higher than the 0.55–5MPa compressive strength obtained for the apparent densities of 0.0397– 0.783 g/cm3, as reported by Ramay et al. [21]. The porous HA showed macropores of 400–600 μm diameters with good pore interconnecting channels. It was also shown that homogeneity of slurry and heating rate affected porosity and density of porous bodies, in turn influencing the compressive strength. More homogeneous slurries and faster heating rate gave porous bodies with the increased compressive strength due to higher apparent density and crystallinity.

Chapter-3

Experimental

3.1. Synthesis of HA by co-precipitation method:

Hydroxyapatite (HA) was prepared by solution-precipitation method using $Ca(NO_3)_2{\cdot}4H_2O$ (Merck, India) and $(NH_4)_2HPO_4$ (Merck, India) as the starting materials and ammonia solution(Merck, india). A suspension of 1M $Ca(NO_3)_2{\cdot}4H_2O$ was prepared at 25^0C. The chemical reaction can be represented as:

$$Ca(NO_3)_2\,4H_2O \;+\; 2NaOH \quad \rightarrow \quad Ca(OH)_2 \;+\; 2\,NaNO_3$$

$$Ca(OH)_2 \xrightarrow{850℃} CaO$$

The Ca:P ratio for stoichiometric HA =1.67. Keeping that ratio constant, the amount of required $(NH_4)_2HPO_4$ was calculated and prepared by dissolving $(NH_4)_2HPO_4$ in DI water. The prepared solution of $(NH_4)_2HPO_4$ was slowly added to the $Ca(NO_3)_2.4H_2O$ solution (in stirring condition) resulting in a turbid solution. The turbidity was removed by adding concentrated HNO_3 which made the solution clear. To the clear solution, 1:1 ammonia solution was drop wise added which resulted in white precipitate of hydroxyapatite. In the experiments the pH was maintained at 10.4.The HA precipitate was continuously stirred for 2 hr. and the precipitate was aged for overnight for settling of the precipitates followed by decantation and removal of ammonia by repeated washing of the precipitate with distilled water. Thie chemical reaction leading to HA formation is as follows:

$$10Ca(NO_3)_24H_2O + 6(NH_4\,)2HPO_4 + 8NH_4OH \;\rightarrow Ca_{10}(PO_4)_6(OH)_2 + 20NH_4NO_3 + \;20H_2O$$

The washing of HA was effected by centrifugation method at a rotational speed of 8000 rpm. The resulting powder was dried at 80^0C and calcined at 850^0Cfor 2 h. The process flow diagram is detailed in Fig 3.1.

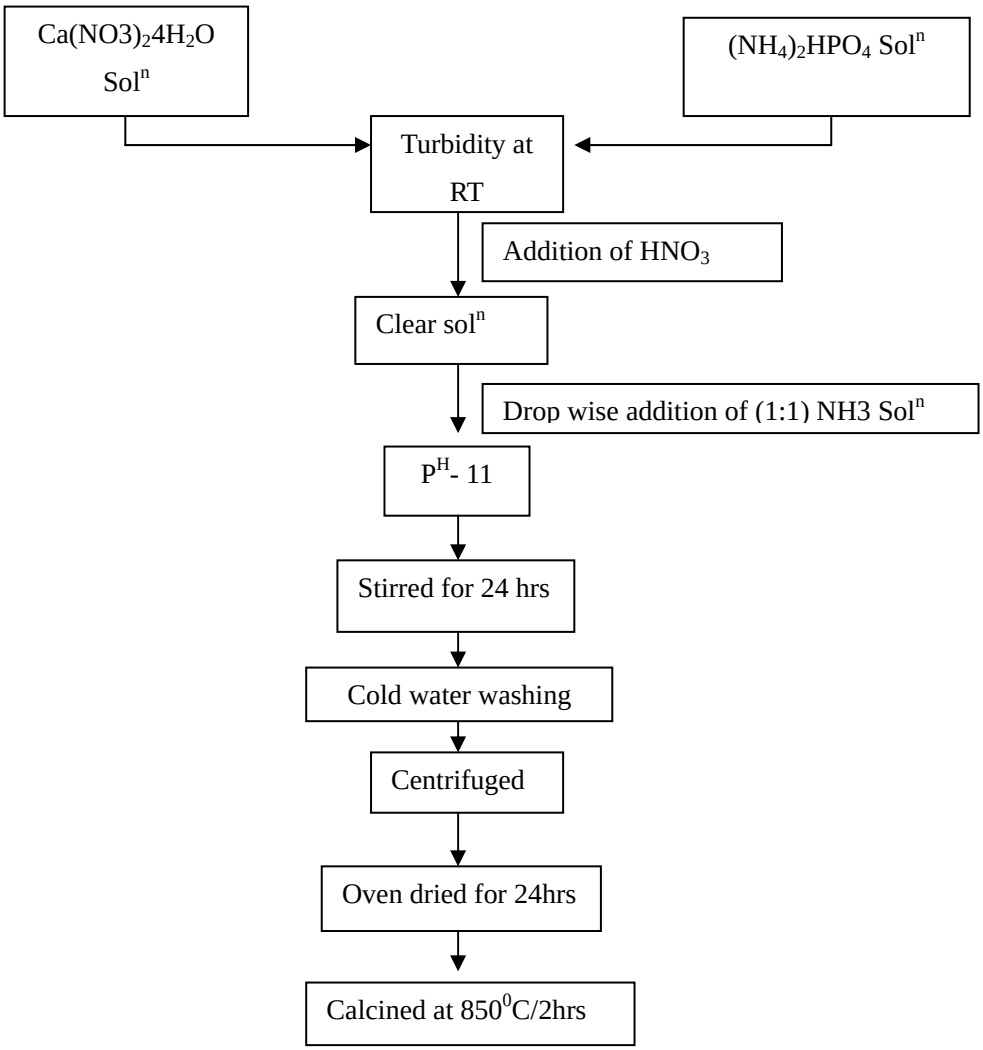

Fig–3.1 Flow chart for the preparation of HA by co-precipitation method

3.2. Processing of porous HA scaffold:

Porous hydroxyapatite was prepared by the following three methods: Polymeric sponge method, Naphthalene as pore former, Polyethylene glycol (PEG) as pore former. The process outline for each of the three methods has been outlined in the following sections:

3.2.1. Polymeric sponge method:

The polymeric sponge method, as it is named, is performed by impregnating porous polymeric substrates (sponges) with HA slurry. The HA slurry containing different weight percent (30, 40, 50%) HA was prepared by dispersing calcined HA powder in water poly vinyl alcohol (PVA) (2, 3, 5 weight %) was added as the binder. Sponge pieces (1×1×1 cm) were pressed into the HA slurry for impregnation. The soaked sponge was oven dried at 80^0C for 24 hours. The dried sponge was sintered at 1250^0C for 4 hour at a heating rate of 3^0C per minute. The samples were kept at 650^0C for one hour for binder burn out. The sintered porous scaffold characterized for strength, porosity, pore size distribution, microstructure, in-vitro ageing tests etc. The process flow chart for fabrication

of porous scaffold by polymeric sponge method was represented as:

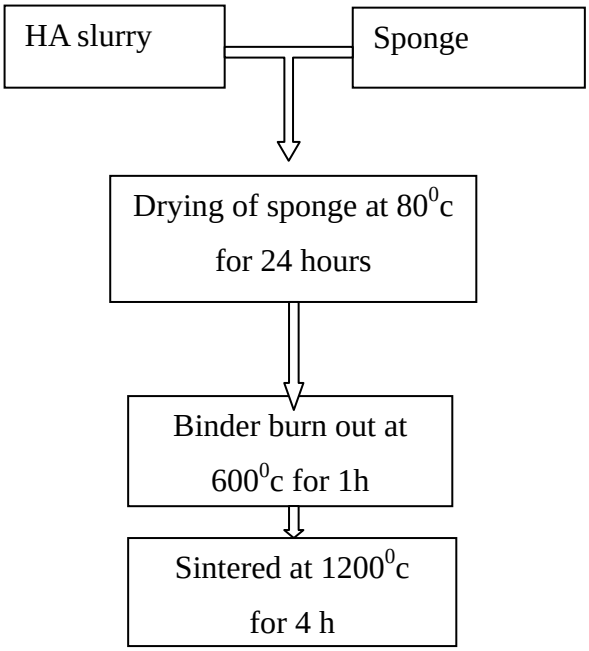

Fig-3.2 Flow chart for fabrication of porous HA scaffold by polymeric sponge method

3.2.2. Porous HA using Naphthalene as pore former:

Weighed amount of calcined HA powder was dry mixed well with naphthalene powder (naphthalene 30, 40, 50 weight %). 5 weight % PVA was added to the dry mixed powder and the powders were wet mixed thoroughly in agate mortar pestle. The dry powder was pressed in a cylindrical die (diameter 12.5 mm). The green pellets were sintered at 1250^{0}C for 4 hours at a heating rate of 3^{0}C per minute. The sintered pellet was characterized as mentioned above. The flow chart for the processing of porous HA scaffold using naphthalene is shown below:

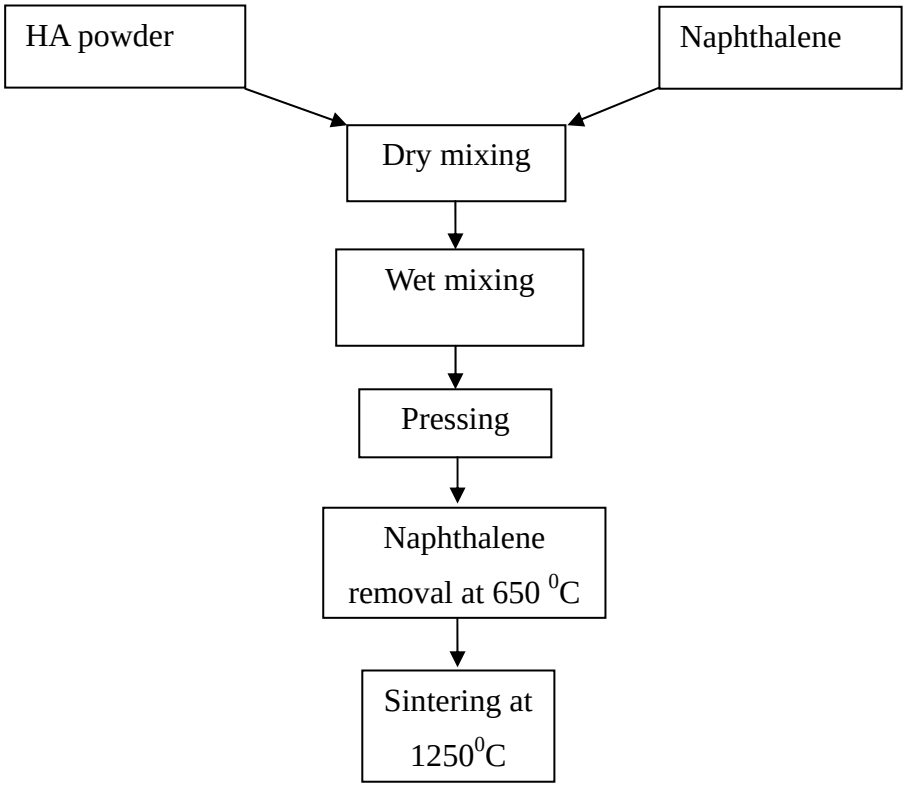

Fig-3.3 Flow chart for fabrication of naphthalene HA scaffold

3.2.3. Porous HA using PEG as pore former:

The calcined HA powder mixed with PEG (PEG4000, PEG6000) in the weight% (40, 30, and 20) with respect to the ceramic to form a HA- PEG slurry. When slurry mixed with PVA to form hydrogel and it was biodegradable. The formation of hydrogel was explained by the following chemical reaction.

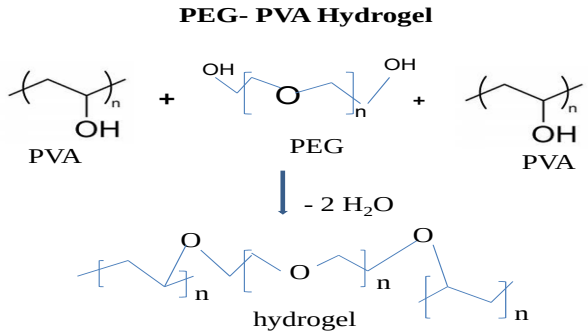

Fig-3.4 formation of PVA-PEG dydrogel

The hydrogel of hydroxyapatite was cast into a glass mould. Molded sample dried at 80^0c for 24 hours. The dried sample was sintered at 1250^0c for 4 hour at the rate of 3^0C per minute. The flow chart for fabrication of HA-PEG scaffold has been represented.

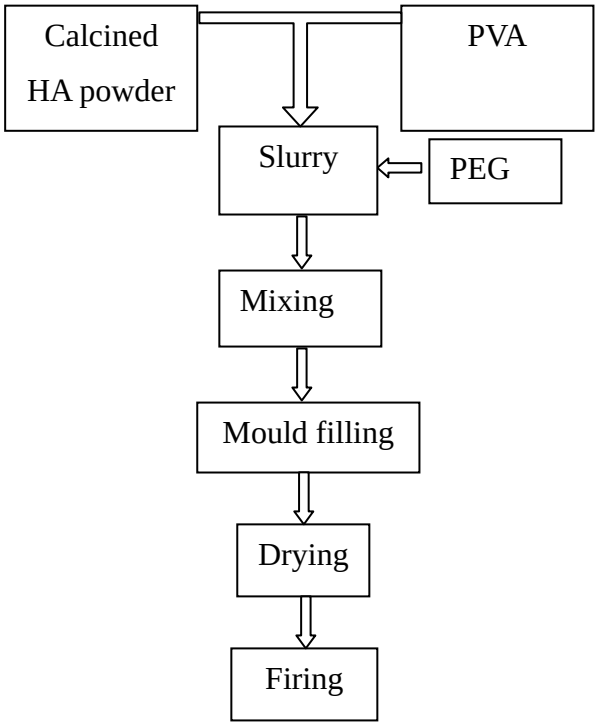

Fig-3.5 Flow chart for fabrication of HA-PEG scaffold

3.3. Characterizations

3.3.1 Phase analysis of HA:

Phase analysis was studied using the room temperature powder X-ray diffraction (Philips PAN analytical Netherland) with filtered 0.154056 nm Cu Kα radiation. Samples are scanned in a continuous mode from 20°- 60° with a scanning rate of 0.04 (degree) / (sec). The HA peaks were identified by referring JCPDS file (reference 74-0565).

3.3.2 Measurement of compressive strength of scaffold:

The compressive strength of the sintered samples was measured by universal testing machine (H10 KS TINIUS OLSEN). The circular pellets (diameter 12.5 mm, thickness) as well as the cubes (1×1×1 cm^3) were broken in compression. The compressive strength of the pellets was determined from the following formula:

For circular pellets

$$Compressive\ strength(\sigma) = \frac{2P}{\pi dt}$$

for cubes

$$compressive\ strength(\sigma) = \frac{P}{A}$$

Where,

P= load in kN

d = diameter of the pellet, t= thickness of the pellet

A= cross sectional area of the cube

3.3.3. Porosity measurement:

Porosity of scaffold was measured by applying Archimedes' principle. Dry weight of sample was taken then samples were kept inside a beaker filled with kerosene and it was kept inside a desiccator for half an hour. Then suspended as well as soaked weight of samples was taken. Apparent porosity and density of sample was represented as:

$$Apparent\ porosity = \frac{S-D}{S-H}$$

$$Bulk\ density = \frac{D \times Density\ of\ kerosene}{S-H}$$

$$Relative\ density = \frac{Bulk\ density}{Theoretical\ density} \times 100$$

Porosity = 1- Relative density

Density of kerosene = 0.81 g/cc

Theoretical density of HA = 3.16 g/cc

Where, D = dry weight

S = suspended weight

H = soaked weight

3.3.4 Mercury Intrusion Porosimetry:

This is a method used to measure both porosity and pore sizes. The scaffolds are placed in a penetrometer and infused with mercury under increasing pressure. As the pressure (P) increases, the radius of pores (r) that can be filled decreases according to the Washburn equation.

$$P = \frac{2\sigma \cos\theta}{r} \qquad (1)$$

Where б is the surface tension of mercury and θ is the contact angle. The open porosity л (porosity accessible to mercury intrusion) is given as

$\pi = V_{intrusion} - V_{scaffold}$, (2)

Where $V_{intrusion}$ is the total intrusion volume of mercury and $V_{scaffold}$ is the volume of the scaffold. The closed porosity ω, porosity not accessible to mercury, can be determined as:

$$\omega = \Pi - \pi. \qquad (3)$$

Where, Π = Total porosity of scaffold.

Applied pressures for mercury intrusion porosimeters range between slightly higher than 0.5 to 60,000 psi.

Scanning electron microscopy (SEM) images are analyzed with various computer software to measure porosity and, particularly, pore sizes.

3.3.5. Bioactivity test:

Bioactivity test was done by taking SBF (simulated body fluid). Simulated body fluids (SBF) prepared in accord with the chemical analysis of human body fluid, with ion concentrations nearly equal to those of the inorganic constituents of human blood plasma, and were used by A.Cuneyt Tas et al. [47].

3.3.5.1 Preparation of SBF solution:

SBF is known to be metastable buffer solutions and even a small, undesired variance in both of the preparation steps and the storage temperatures, may drastically affect the phase purity and high-temperature stability of the produced HA powders, as well as the kinetics of the precipitation processes.

Merck-grade NaCl (99.5%), $NaHCO_3$ (99.5%), KCl (99.0%), Na_2HPO_4 $2H_2O$ (99.5%), $MgCl_2$ $6H_2O$ (99.0%), Na_2SO_4, $(CH_2OH)_3CNH_2$ (99.5%), $CaCl_2H_2O$ (99.0%) and HCl (37 vol%) were used in the preparation of the SBF of this study.

Table -3.1 Chemical composition of SBF solutions: [37]

Order	Reagent	Amount (gpl)
1	NaCl	6.547
2	$NaHCO_3$	2.268
3	KCl	0.373
4	Na_2HPO_42H2O	0.178
5	$MgCl_2$ $6H_2O$	0.305
6	$CaCl_2$ $2H_2O$	0.368
7	Na_2SO_4	0.071
8	$(CH_2OH)_3CNH_2$	6.057

SBF solutions were prepared by dissolving appropriate quantities of the above chemicals in deionized water. Reagents were added, one by one after each reagent was completely dissolved

in 700 ml of water, in the order given in Table-3.1. A total of 40 ml of 1 M HCl solution was consumed for pH adjustments during the preparation of 1 Ltr. of SBF solutions. A 15 ml aliquot of this acid solution was added just before the addition of the sixth reagent, i.e. $CaCl_2$ $2H_2O$. Otherwise, the solution would display slight turbidity. The remaining part of the HCl solution was used during subsequent titration. Following the addition of the eighth reagent (tris (hydroxymethyl) aminomethane), the solution temperature was raised from ambient to 37^0C. This solution was then titrated with 1 M HCl to a pH of 7.4 at 37^0C. During the titration process, the solution was also continuously diluted with consecutive additions of de-ionized water to make the final volume equal to 1 Ltr. It was observed in this study that the prepared SBF solutions can be stored at 5^0C for a month without degradation.

Table-3.2: Ion concentrations of SBF solutions and human plasma:[37]

Ion	Kokubo et al. (mM)	Present work (mM)	Human plasma (mM)
Na^+	142.0	142.0	142.0
Cl^-	147.8	125.0	103.0
HCO_3^-	34.2	27.0	27.0
K^+	5.0	5.0	5.0
Mg_2^+	1.5	1.5	1.5
Ca_2^+	2.5	2.5	2.5
HPO_4^{2-}	1.0	1.0	1.0
SO_4^{2-}	0.5	0.5	0.5

3.3.6. Biodegradation test:

Biodegradation test of porous scaffold was done by taking Tris-HCl buffer solution. 0.05MTris- HCl solution was prepared using distilled water. The pH of solution was maintained 7.4 at 37^0c by adding 1MHCl. Scaffolds were soaked in Tris-HCl buffer solution for one week then the samples were dried at 120^0c and final weight of sample was taken.

$$\%\, weight\ loss = \frac{W_0 - W_t}{W_0} \times 100$$

Where, W_0 = initial weight of sample

Wt = final weight of sample after soaking in Tris-HCl solution

3.3.7. Microstructure analysis by SEM:

Surface morphology, pore shape and pore size distribution was studied by SEM (Jeol JSM 6480LV). Tissue growth and bioactivity of SBF treated samples were studied by SEM attached with Energy-Dispersive X-Ray (EDX). The SEM images of platinum coated sintered scaffold were observed in secondary electron ray at 15KV.

Chapter-4

Results and discussion

4.1. Phase analysis of sintered HA:

Fig–4.1 shows the XRD pattern of sintered HA prepared by co-precipitation method. The HA peaks were identified by referring JCPDS files (74-0565) and the XRD pattern was shown below:

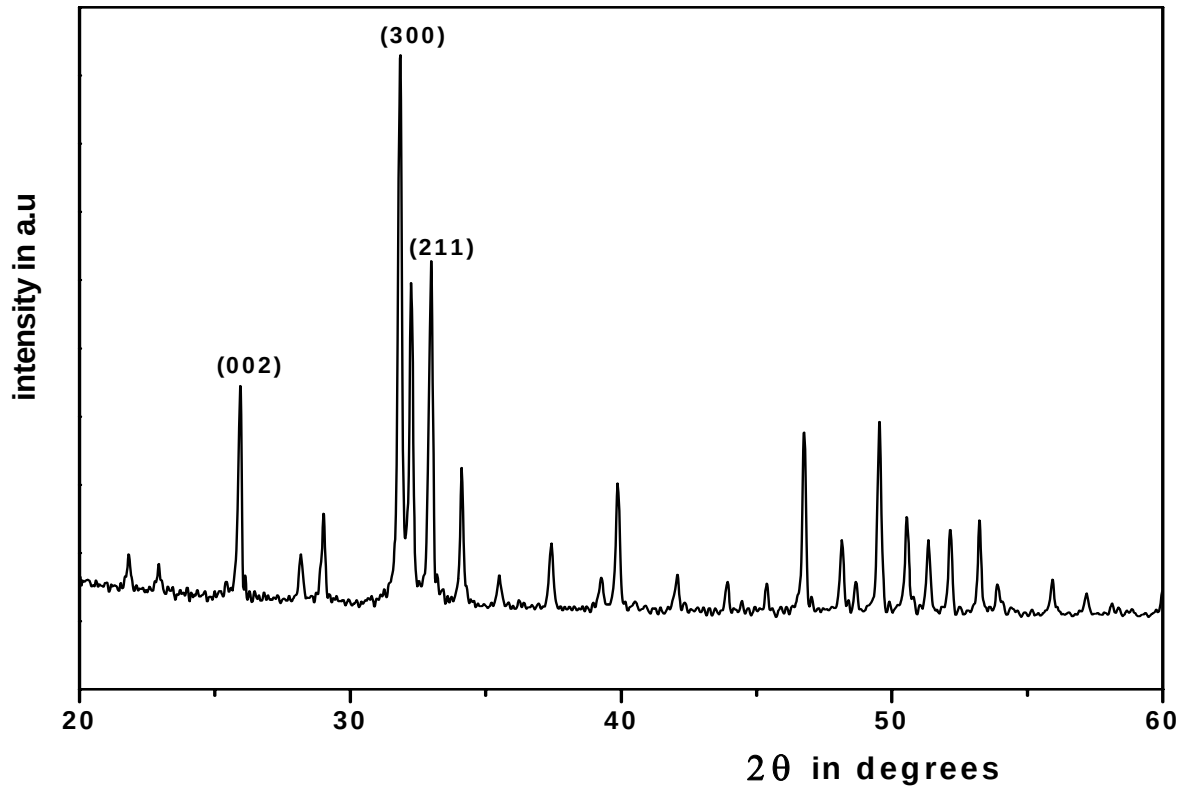

Fig-4.1 XRD pattern of sintered HA at1250^{0}c

The XRD pattern shows that the calcined powder contains only hydroxyapatite (marked by peaks at d= 3.4496, 2.8199, 2.7229) peaks. All other peaks also correspond to HA and no extra peaks were found. Thus the synthesized HA powder was phase pure at1250^{0}c without decomposition to β-TCP.

4.2. Bulk Density, Porosity and Strength of porous HA scaffolds prepared by polymeric sponge method:

Table -4.1: Effect of PVA on the bulk density, porosity and strength for 40% HA loading.

PVA (wt. %)	BD (gm/cc)	Apparent Porosity (%)	Compressive Strength (MPa)
2	0.9238	70.76	0.69
3	1.035	67.08	0.82
5	1.16	62.16	1.02

The effect of PVA concentration on the bulk density, strength and porosity of HA scaffold is shown in Table-4.1.This table indicates that for a fixed HA concentration (40%), the porosity is inversely proportional to PVA concentration. This is due to the fact that increasing the PVA amount causes grater gel formation which increases the strength of green body which turn increases the fired strength. The gels also being lyophilic cause a reduction in porosity.

Table-4.2: **Effect solid loading (at 3 wt% PVA concentration) on the porosity, bulk density and strength HA scaffold.**

HA (wt. %)	BD (gm/cc)	Apparent Porosity (%)	Compressive Strength (MPa)
40	1.03	67.08	0.82
50	1.37	56.51	0.85

Table – 4.2 shows the effect of solid loading (at 3 wt% PVA concentration) on the bulk density, porosity and strength of HA scaffolds prepared from polymeric sponge method. It is seen that on increasing the solid loading from 40 to 50 wt% the bulk density and strength increases while the porosity decreases.

Fig-4.2 sintered hydroxyapatite scaffold prepared by polymeric sponge method.

4.3. Bulk density, porosity and strength of porous HA scaffolds prepared using PEG-PVA:

Table-4.3: Effect of PEG 4000 concentration on HA- PEG scaffold.

PEG-4000 (wt. %)	BD (gm/cc)	Apparent Porosity (%)	Compressive Strength (MPa)
20	2.01	36.39	3.97
30	1.69	46.49	2.31
40	1.35	51.66	1.43

Table-4.3. shows bulk density, porosity and strength of HA-PEG4000 scaffold. It has been seen that an increase in the concentration of PEG-4000 contents, the bulk density decreases, porosity increases and strength decreases.

Table-4.4: Effect of PEG 6000 concentration on HA-PEG scaffold

PEG-6000 (wt. %)	BD (gm/cc)	Apparent Porosity (%)	Compressive Strength (MPa)
20	1.84	41.67	3.39
30	1.91	39.32	3.97
40	1.98	37.24	4.54

Table-4.4 shows the effect of PEG6000 concentration on the bulk density, porosity and strength of HA-PEG6000 scaffold. It has been seen that with decrease in the PEG6000 contents the bulk density decreases, porosity increases and strength decreases. The above results could be explained as follows:

The effectiveness of PEG on the pore formation depends on oxidizable hydroxyl value (OHV). The OHV for PEG4000 in the range 22.5-29.5 while that for PEG6000 in between 17.5-20. This implies that for lower molecular weight PEG (PEG4000) higher porosity will be obtained when enough mass of PEG is present. However for high molecular weight PEG, the available contents of PEG additive in the mixture have to decrease[48]. This can also be explained from the Kamide's diffusion theory of PEG which says that a PEG with a lower molecular size has higher diffusivity while it is lower for high molecular weight PEG. Thus increasing the concentration of high molecular weight PEG further causes problem in diffusion and hence porosity decreases.

Fig-4.3 PEG-HAP scaffold sintered at 1250^{0}C

4.4 Bulk density, porosity and strength of porous HA scaffold using naphthalene and 5% PVA:

Table-4.5: Effect of naphthalene concentration on HA-naphthalene scaffold with PVA 5 wt %

Naphthalene (wt. %)	BD (gm/cc)	Porosity (%)	Compressive Strength (MPa)
30	2.38	25.27	11.44
40	2.12	32.84	10.28
50	1.95	38.19	8.92

Table-4.6 shows the effect of naphthalene concentration on the porous HA-naphthalene scaffold. It has been observed that as the naphthalene concentration increases the bulk density decreases, porosity increases and strength decreases.

Table-4.6: porous HA scaffold using naphthalene-PVA(5wt.%) system in which naphthalene is dissolved in benzene.

Naphthalene (wt. %)	BD (gm/cc)	Apparent Porosity (%)	Compressive Strength (MPa)
30	2.14	32.24	10.18
40	1.92	39.32	8.84
50	1.5	52.46	7.01

Table -4.6 shows porous HA scaffold using naphthalene PVA system in which naphthalene dissolved in benzene. This was done to maintained uniform distribution of naphthalene in HA. It has been observed that with increasing naphthalene contents the porosity increases, bulk density decreases and strength decreases as compared to the naphthalene-PVA scaffold.

4.5. Microstructure of the scaffold structure:

Fig -4.5 shows the SEM images of porous HA scaffolds prepared from polymeric sponge method with varying HA and PVA contents. It has been seen that macropore were inter connected through cell walls. The SEM images were shown as:

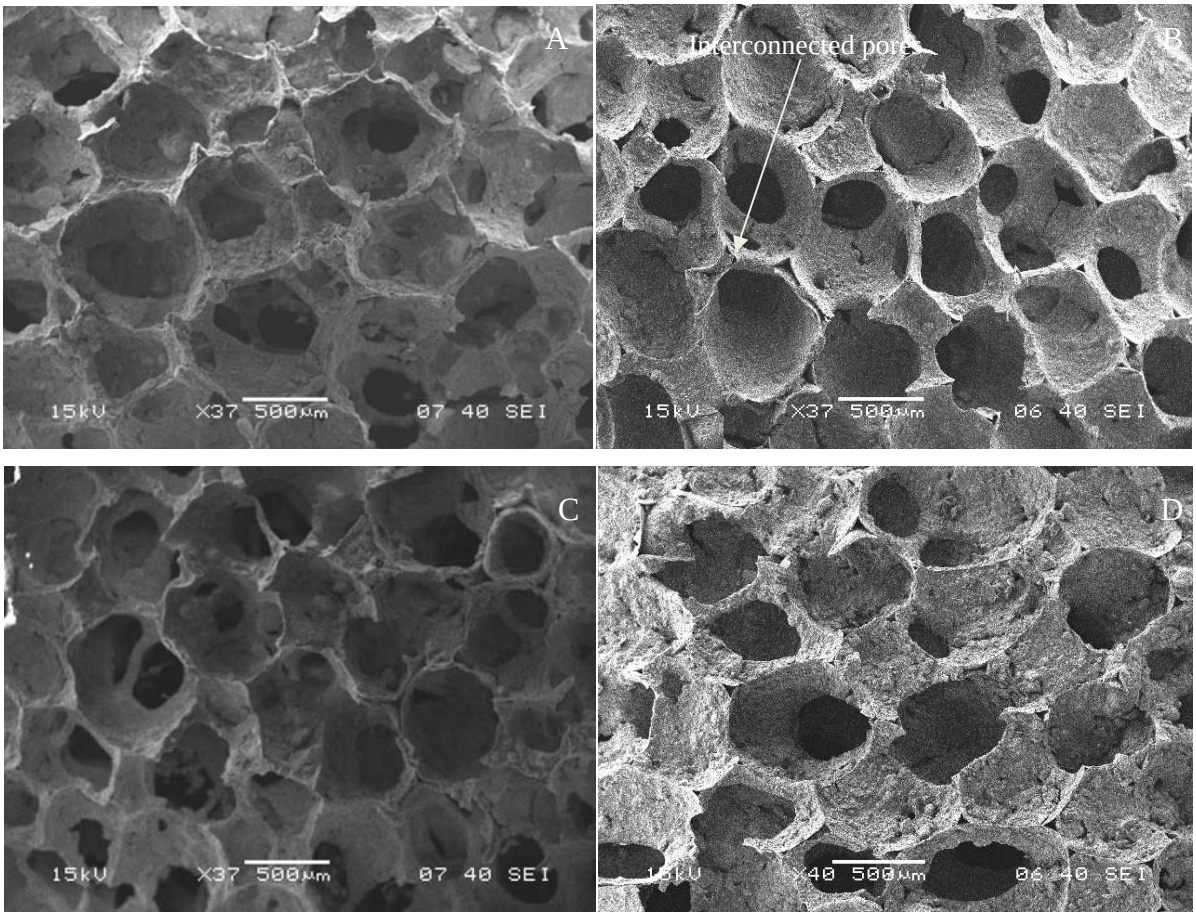

Fig- 4.5 SEM images of HA scaffolds prepared from polymeric sponge method (A) 40 wt% HA & 2 wt %PVA, (B) 40 wt % HA & 3 wt % PVA, (C) 40 wt % HA & 5 wt % PVA, (D) 50 wt % HA & 3 wt % PVA

From the SEM image it was observed that pore size of HA scaffold in the range ~ 400 – 500 µm and pores were well interconnected. The concentration of PVA and HA affect the pore size, porosity, pore inter connectivity as well as strength of scaffold. Image (B) has well interconnected pores with pore diameter ~500µm.

Fig-4.6 shows the SEM images of PEG-HA scaffold. It has been seen that pores were not well interconnected porous HA-PEG scaffold. Micro and macropores were observed in the surface of scaffold. The SEM images were shown bellow as:

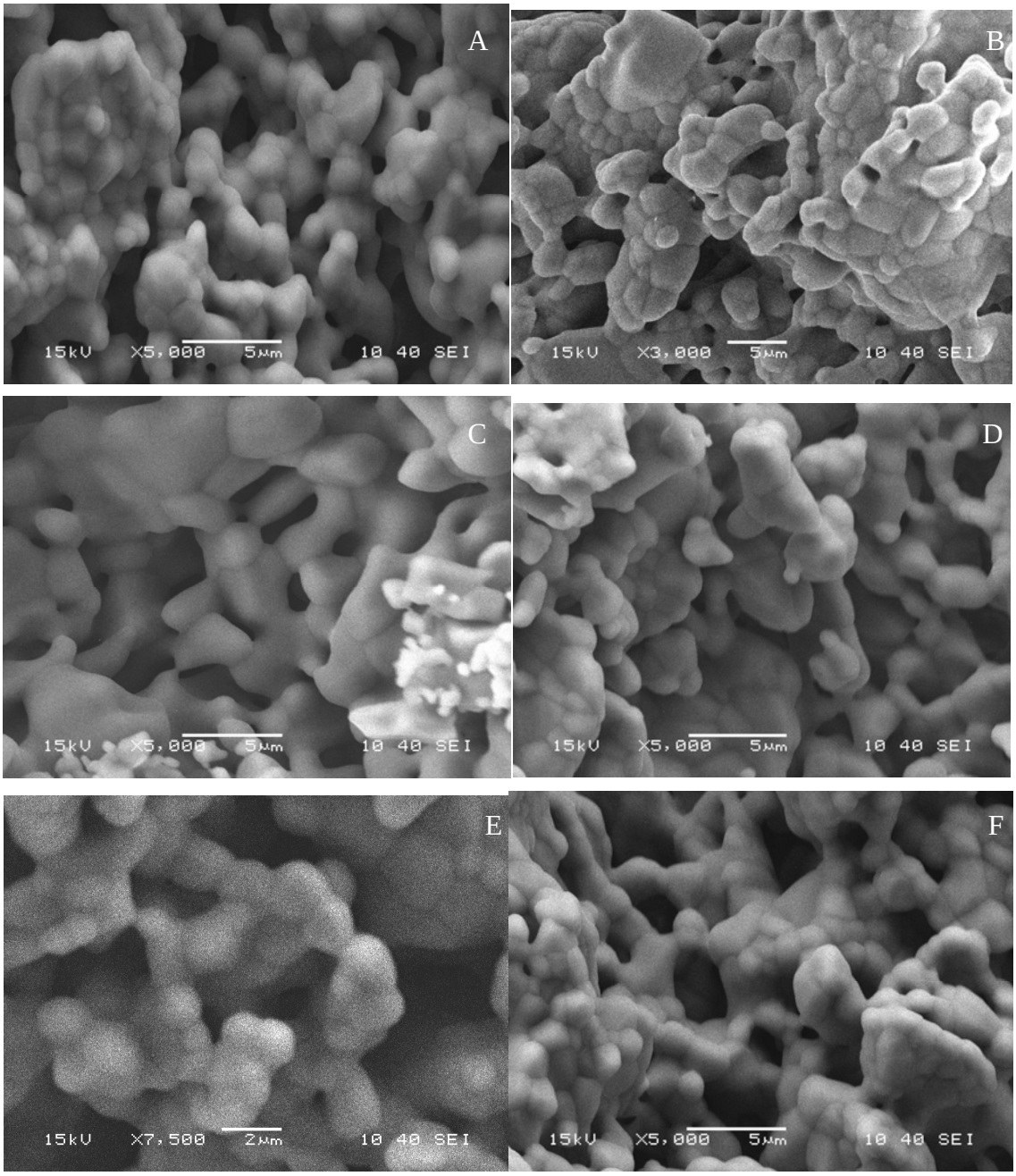

Fig-4.6 SEM of HA- PEG scaffold, (A) PEG4000 -20 wt %, (B) PEG4000 – 30 wt %, (C),(D), (E),& (F) PEG6000- 40, 30, 20,& 10 wt % respectively.

From the SEM image of HA – PEG scaffold it was observed that the porosity and pore size of the scaffold depends on the molecular weight and weight % of PEG in the scaffold. Higher the molecular weight of PEG, lower weight % of HA required for higher porosity.

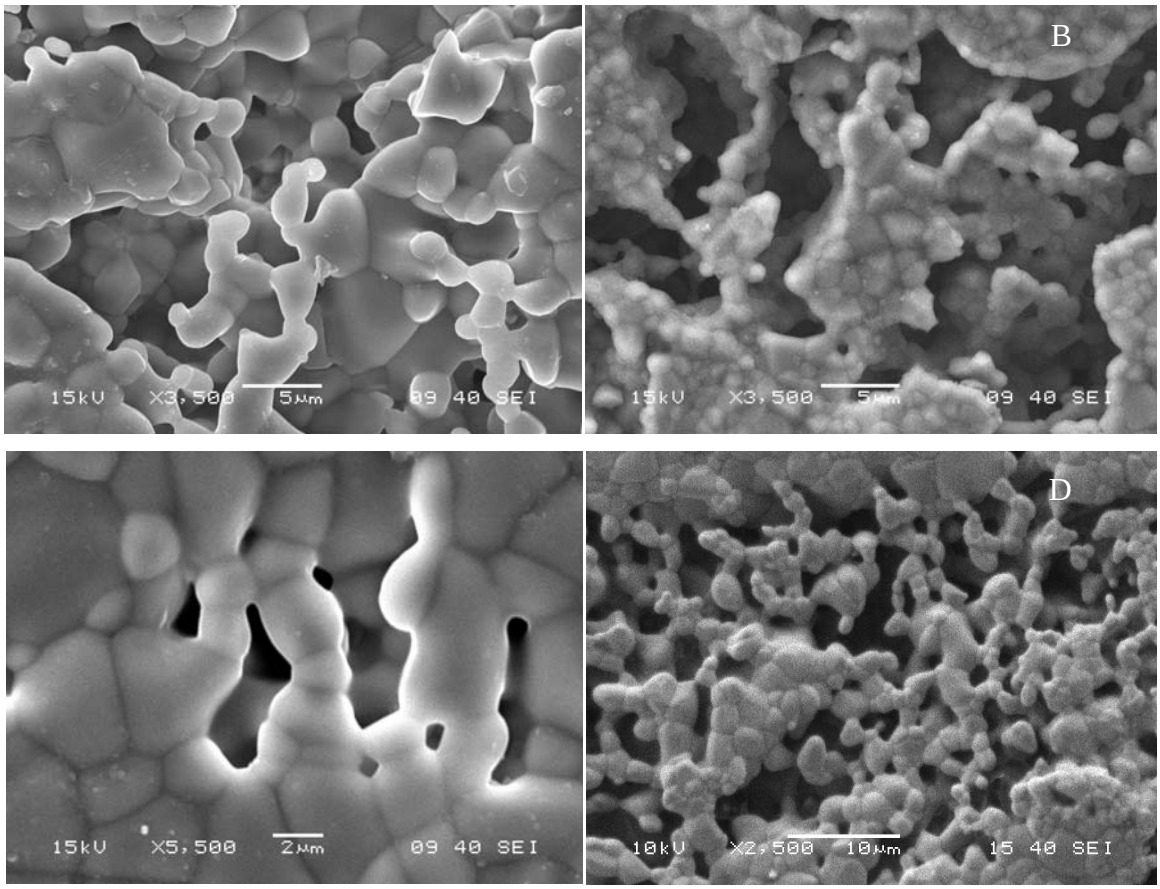

Fig-4.7 SEM image of HA – naphthalene scaffold, (A) & (B) naphthalene 30 & 50wt %, (C) & (D) naphthalene in benzene 30 & 50 wt %

From the SEM image of HA-naphthalene scaffold it has been observed that pores were not properly interconnected. Pore size also depends upon the size and weight of pore former. When naphthalene dissolved in benzene solution higher porosity was obtained with uniform pore size distribution. Benzene, an organic solvent, developed porosity and maintained uniformity between pores.

4.6. Pore size distribution of scaffold:

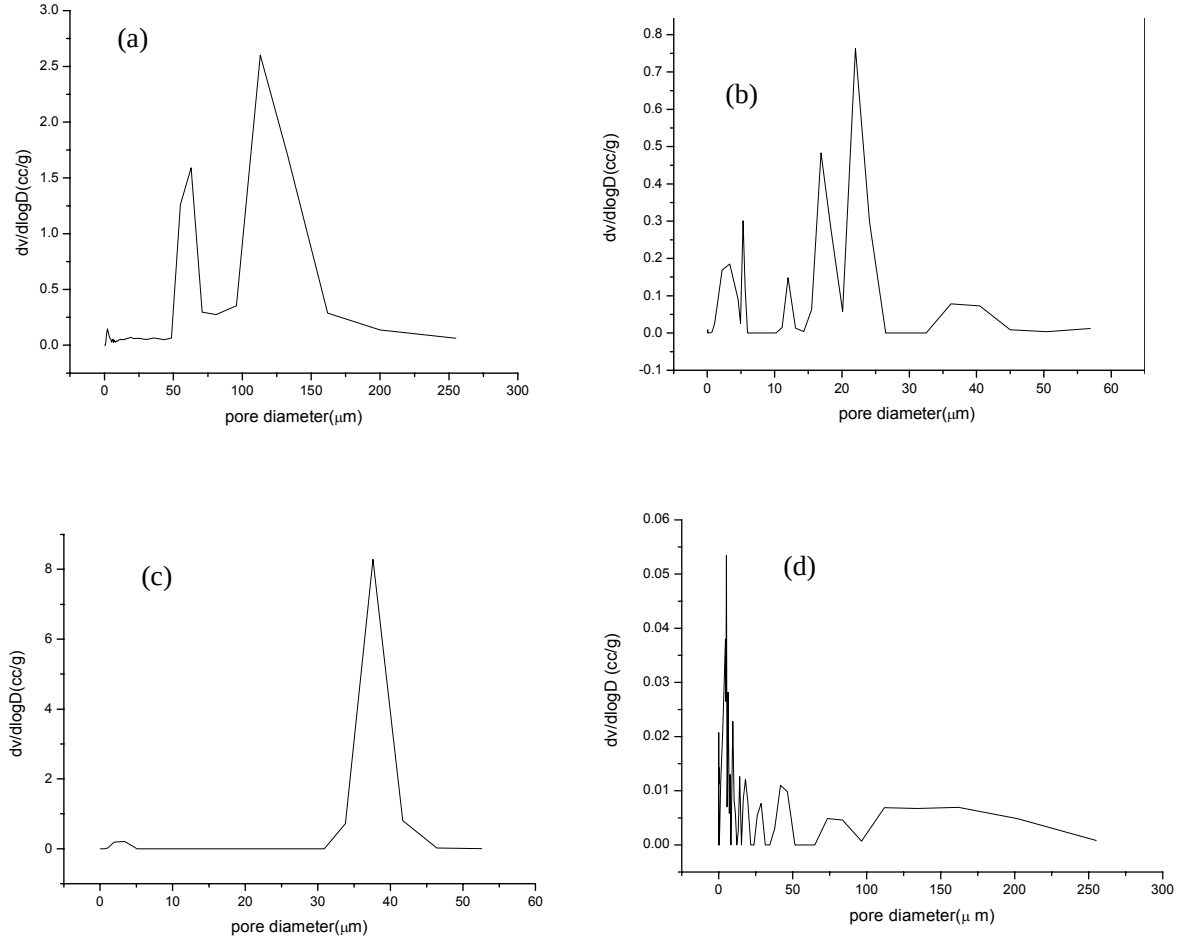

Fig-4.8 Hg- distribution of scaffolds, (a) HA scaffold from polymeric sponge method with HA 40 wt% & PVA 3 wt%, (b) HA- PEG scaffold with PEG4000 – 20 wt%, (c) HA-PEG scaffold with PEG6000- 30 wt%, (d) HA-naphthalene scaffold with naphthalene 50 wt%

Fig- 4.8 shows the pore size distribution and pore size of HA scaffold. HA scaffold obtained from polymeric sponge method with porosity 68% and pore size with the range 125 μm and some pores also found in the range 50 μm. Fig-4.8 (b) has multimodal peaks that shows a range of porosity from 10-25 μm. PEG6000 has single modal peak with pore size 40μm. HA-naphthalene scaffold has multimodal peaks which shows a range of porosity from 5- 50 μm. Maximum fraction of pore were in the range of 10- 15μm. The large pores in the polymeric sponge method could not be detected by Hg-porosimeter.

From the above pore size distribution data it can be seen that the best possible pore size distribution obtained from polymeric sponge method along with the interconnected pores. In PEG-HA scaffold the pore size is very small for tissue connectivity. The pore size distribution of fig-4.8 (b),

(c) and (d) were varying due to the different processing methods adapted while in polymeric sponge method the HA was made in the slurry and deep into the polymeric sponge, other methods, the pore former either in the powder or solution. Therefore sample (b) & (d) proper optimization of the processing of scaffold required.

4.7 In-vitro bioactivity:

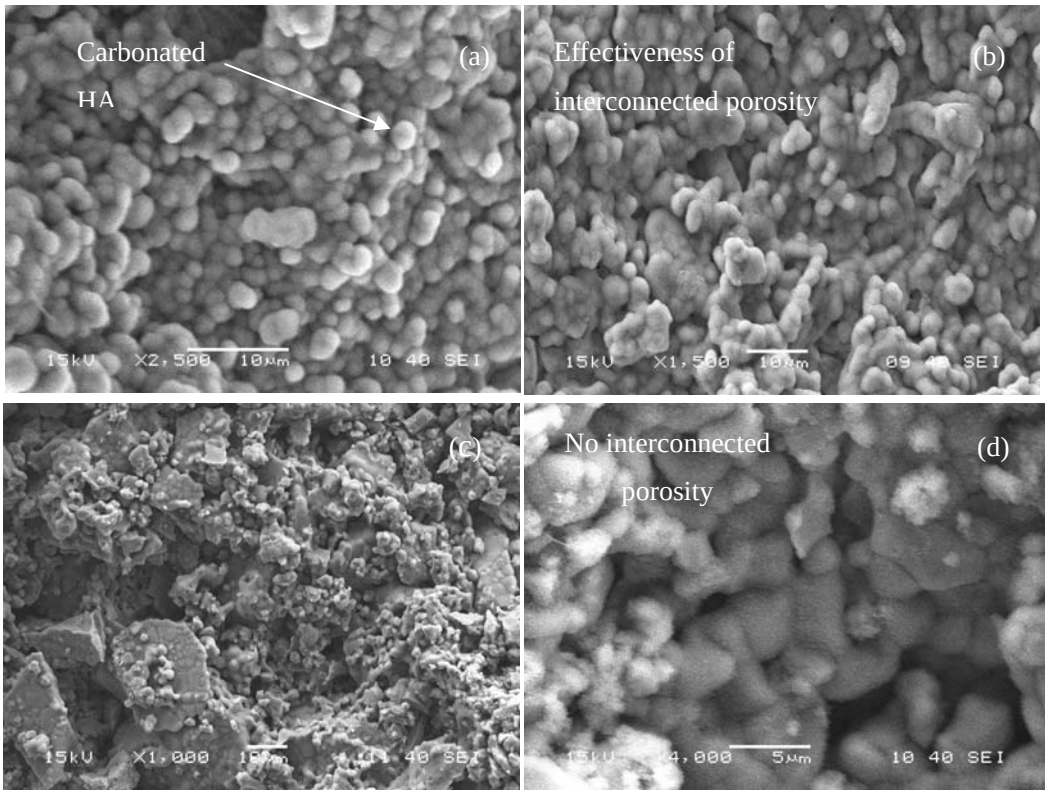

Fig-4.9 SEM images of HA scaffold 7 day soaked in SBF solution, (a) & (b) HA – polymeric sponge scaffold, (c) HA- PEG scaffold, (d) HA- naphthalene scaffold

The SEM of HA scaffold after being soaked in SBF solution for 7 days shows that carbonated HA grows on the surface of porous scaffold and tissue growth was higher in HA scaffold from sponge method as compared to HA- PEG and HA- naphthalene samples. The tissue growth takes place rapidly in porous HA scaffold prepared from polymeric sponge method, due to effectiveness of interconnected porosity but in PEG-HA and HA-naphthalene scaffolds were no interconnected porosity. Thus, in dense samples tissue growth takes place slowly. In porous form the surface area is greatly increases which allow more tissue to be carried as compared to dense HA.

When porous HA is treated in SBF solution, at first, on soaking in SBF, the surface structural change occurs in HA resulting in the formation of a Ca-rich ACP on their surfaces. In view of change in Ca/P ratio, the formation of Ca-rich ACP is a consequence of interaction of the HA surface specifically with the calcium ions in the SBF. The second surface structural change is the formation

of Ca-poor ACP, for which the HA appear to use the Ca-rich ACP on their surfaces to interact with the phosphate ion in the fluid. The third surface structural change is the formation of apatite. The Ca-poor ACP on the HAs appears to gradually crystallize into bonelike apatite, through which the HA appear to stabilize their surfaces in SBF [36].

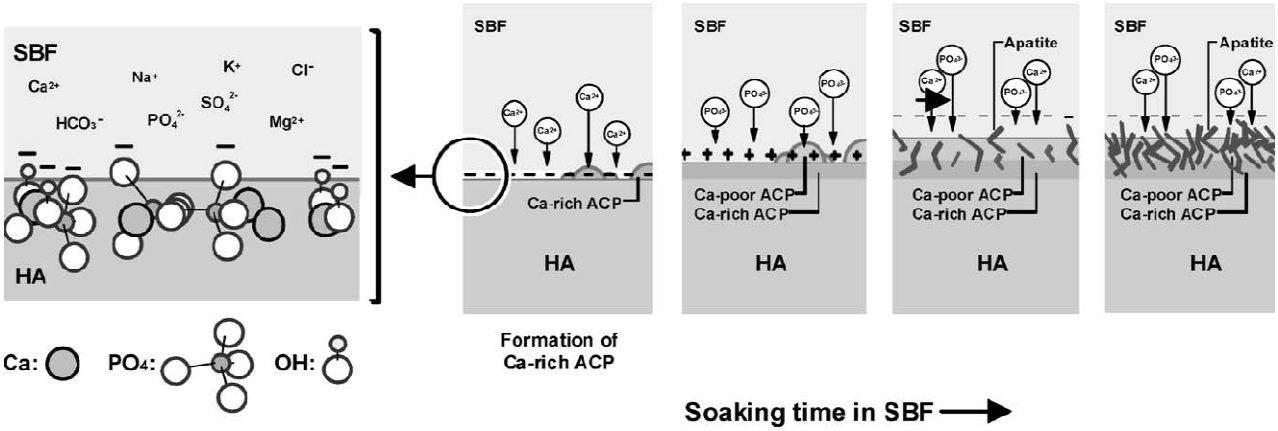

Fig-4.10 Schematic presentations of the origin of negative charge on the HA surface and the process of bonelike apatite formation thereon in SBF

4.8. In-vitro Biodegradation:

Biodegradation of porous samples were carried out in Tris-HCl solution. HA samples were soaked in Tris-buffer solution at pH 7.4 and temperature 37^0C for 7 days [26]. When porous HA was soaked in Tris-buffer solution, the loss of calcium ion took place which resulted in the increase in pH of the buffer from 7.4 to 8.2 which confirms the biodegradation of scaffolds. In the porous HA scaffolds prepared from sponge method, 5 % weight loss was observed but for HA-PEG and HA-naphthalene scaffold it was 4.1 and 3.8 % weight loss respectively. Thus the weight loss was higher for the scaffold which has higher porosity and it appears that the ageing time in Tris-HCl solution may also affect the weight loss behavior.

Chapter-5

Conclusions

Conclusions:

- The HA prepared from $CaNO_3 4H_2O$ and $(NH_4)_2HPO_4$ by co-precipitation method was phase pure at temperature 1250^0C without appearance of β-TCP phase.
- The porous scaffolds were prepared from sponge method and use of pore former PEG and benzene.
- Porous HA prepared from polymeric sponge method had about 70% porosity having pore diameter ~400-500 μm and the pores were inter-connected.
- With increase in PVA contents from 2 to 5 wt% with 40% solid loading, the strength of the scaffold increased from 0.69-1.02 MPa.
- The pore size and pore inter connectivity depended upon the slurry viscosity and solid loading but in HA-naphthalene scaffold the porosity and pore interconnectivity depended upon the amount of pore former used.
- Porosity and pore size uniformity increases in HA-naphthalene scaffold when naphthalene dissolved in benzene.
- In HA-naphthalene scaffolds, a range of porosity (25-50%), could be obtained by varying naphthalene contents obtained and the scaffolds had a compressive strength between 7-10MPa.
- In HA-PEG 4000 scaffold, the porosity increased with an increase in PEG 4000 content, while it decreased for PEG 6000. This was due to the difference in the OHV (oxidizable hydroxyl value) of the two polymers.
- In PEG-HA scaffold, a range of porosity (38-50%), pore diameter (5-60 μm) and compressive strength (1.45-4.5 MPa) was obtained by varying the PEG contents. For proper tissue growth, the minimum diameter required for the pore is >140μm.
- In-vitro studies of bioactivity and biodegradability show that rate of tissue growth and resorbtion takes place rapidly in those scaffold which having high porosity.
- Pore size and porosity depended upon the amount of pore former and sintering temperature. It also seen that range of porosity from 1-100 μm obtained by varying the amount and size of ceramic and PEG particles. Molecular weight of PEG plays an important role in the morphology, structure and pore size of scaffold.

References:

[1] Groeneveld E.H, Van den Bergh J.P, Holzmann P, Ten Bruggenkate C.M, Tuinzing D.B, Burger E.H. Mineralization processes in de-mineralized bone matrix grafts in human maxillary sinus floor elevations. J BiomedMater Res 1999; 48(4):393–402

[2] Kuboki Y, Takita H, Kobayashi D, Tsuruga E, Inoue M,Murata M, et al. BMP-induced osteogenesis on the surface of hydroxyapatite with geometrically feasible and non-feasible structures: topology of osteogenesis. J BiomedMater Res 1998; 39(2):190–9

[3] Hulbert S.F, Young F.A, Mathews R.S, Klawitter J.J,Talbert C.D, Stelling F.H. Potential of ceramic materials as permanently implantable skeletal prostheses. J BiomedMater Res 1970;4(3):433–56.

[4] Leony Leon C.A.New perspectives in mercury porosimetry. Adv Colloid Interface Sci 1998;76–77:341–72.

[5] Itala AI, Ylanen H.O, Ekholm C, Karlsson K.H, Aro H.T. Pore diameter of more than 100 micron is not requisite for bone ingrowth in rabbits. J BiomedMater Res 2001;58(6):679–83.

[6] R.A.Whiite, J.N.Weber, and E.W.White, “Replamineform:A new process for preparing porous ceramics, metal and polymer prosthetic materials,” science, 176, 922-24 (1972).

[7] D.m.Ray, W. Eysel, and D. Dinger, “hydrothermal synthesis of various carbon containing calcium hydroxyapatite,” Matter.Res. Bull, 9, 35 (1974).

[8] K.A .Hing, S.M.Best, and W. Bonfield, “characterization of porous hydroxyapatite,” J. Matter. Med, 10,135-45 (1999).

[9] B.V. Rejda, J.G.Peelen, and k.de Groot, “tricalcium phosphate as bone substitute” J. Bioeng.1, 93-97 (1977).

[10] H. Arita, V.M. Castono, and D.S Wilkinson, “synthesis and processing of hydroxyapatite ceramic tapes with controlled porosity” J. Mater.Sci. :Matter Med.,6, 19-23 (1995).

[11] Yasuki, “preparation of adsorption catalyst marerial” Jpn. Pat. No. 09108567, 1995.

[12] L. M. Rodriguez-Lorenzo, J.M.F. Ferreira, and M. Vallet-Regi, “processing of porous hydroxyapatite by starch consolidation”

[13] O.Richart, M.Descamps, and A.Liebetrau, “macroporous calcium phosphate caramics”, 2001

[14] J.Saggio-Woyansky, C.E.Scoott, and W.P.Minner, “processing of porous ceramics,” Am. Ceram .Soc. Bull, 71[11] 1674-82 (1992).

[15] D.C.Tancred, B.A.O.Mccormark, “A synthetic bone implant macroscopically identical to cancelous bone” Bio materials,19, 2303-11 (1998).

[16] A.S.Rebeiro, and R.L.Reis, “two new routes for producing bioactive ceramics: polyurethane precursor and microwave backing” vol 11, New York,1998.

[17] P.Sepulveda, J.G.P.Binner,S.o Rogero “production of porous hydroxyapatite by a gel casting of foams” J.Biomed.Mater.Res. 50, 27-34 (2000).

[18] Kuboki Y, Takita H, Kobayashi D, Tsuruga E, Inoue M, Murata M, et al. BMP-induced osteogenesis on the surface of hydroxyapatite with geometrically feasible and non-feasible structures: topology of osteogenesis. J BiomedMater Res 1998;39(2):190–

[19] Harvey EJ, Bobyn JD, Tanzer M, Stackpool GJ, Krygier JJ, Hacking SA.Effect of flexibility of the femoral stem on bone remodeling and fixation of the stem in a canine total hip arthroplasty model without cement. J Bone Joint Surg Am 1999; 81(1):93–107.

[20] Chang YS, Gu HO, Kobayashi M, Oka M. Influence of various structure treatments on histological fixation of titanium implants. J Arthroplasty 1998; 13(7):816–25.

[21] D Lima D.D, Lemperle SM, Chen PC, Holmes RE, Colwell Jr CW. Bone response to implant surface morphology. J Arthroplasty 1998; 13(8):928–34.

[22] Steflik DE, Corpe RS, Young TR, Sisk AL, Parr GR.The biologic tissue responses to uncoated and coated implanted biomaterials. Adv Dent Res 1999; 27–33.

[23] Simon J.L, Roy T.D, Parsons J.R, Rekow E.D, Thompson V.P, Kemnitzer J, et al. Engineered cellular response to scaffold architecture in a rabbit trephine defect. J Biomed Mater Res A 2003; 66(2):275–82.

[24] L.L. Hench, J. Wilson, An Introduction to Bioceramics, World Scientific, Singapore, 1993.

[25] L.L Hench, Biomaterials 19 (1998) 1419

[26] Soon-Ho Kwon, Youn-Ki Jun, Seong-Hyeon Hong, In-Seop Lee, and Hyoun-Ee Kim; “Calcium phosphate bioceramics with various porosities and dissolution rate” J. Am. Ceram. Soc, 85[12] 3129-31(2002).

[27] Shi Hong Li, Joost R. de Wijn, Pierre Layrolle, and Klaas de Groot; “Novel method to manufacture porous hydroxyapatite by Dual- Pha0se mixing” j. Am. Ceram. Soc, 86[1] 65-72 (2003).

[28] K.Schwartzwalder and A. V. Sommers, US patent No. 3090094, may 21 (1963).

[29] Zhu, X., Jiang, D. and Tan, S., “The control of slurry rheology in the processing of reticulate porous ceramics”. *Mater. Res. Bull.*, 2002, **37**, 541–553.

[30] Pu, X., Liu, X., Qiu, F. and Huang, L., “Novel method to optimize the structure of reticulated porous ceramics”. *J. Am. Ceram. Soc.*, 2004, **87**(7), 1392–1394.

[31] Lin, K., Chang, J., Zeng, Y. and Qian, W., “Preparation of macroporous calcium silicate ceramics”. *Mater. Lett.* 2004, **58**, 2109–2113.

[32] Nursen Koc, Muharrem Timuc in, Feza Korkusuz,” Fabrication and characterization of porous tricalcium phosphate ceramics” Ceramics International 30 (2004) 205–211

[33] Han Guo , Jiacan Su , Jie Wei , Hang Kong , Changsheng Liu; “Biocompatibility and osteogenicity of degradable Ca-deficient hydroxyapatite scaffolds from calcium phosphate cement for bone tissue engineering” Acta Biomaterialia 5 (2009) 268–278.

[34] YueJun Tang, YueFeng Tang , ChunTang Lv , ZhongHua Zhou; “Preparation of uniform porous hydroxyapatite biomaterials by a new method,” Applied Surface Science 254 (2008)

5359–5362.

[35] Marek Potoczek; “Hydroxyapatite foams produced by gelcasting using agarose” Materials Letters 62 (2008) 1055–1057.

[36] Hyun-Min Kima, Teruyuki Himeno, Tadashi Kokubo, Takashi Nakamura; “Process and kinetics of bonelike apatite formation on sintered hydroxyapatite in a simulated body fluid” Biomaterials 26 (2005) 4366–4373.

[37] A. Cuneyt Tas, “Synthesis of biomimetic Ca-hydroxyapatite powders at 37^0C in synthetic body fluids” Biomaterials 21 (2000) 1429}1438.

[38] Deville, Saizaa and Tomsia, Freeze casting of porous hydroxyapatite scaffolds for bone tissue engineering, 2006.

[39] Itatani K, Uchino T, Okada I, Preparation of Porous Hydroxyapatite Ceramics from Hollow Spherical Agglomerates Using a Foaming Agent of H2O2, 2003.

[40] Lyckfeldt, O. and Ferreira, J. M. F., Processing of porous ceramics by starch consolidation. J. Eur. Ceram. Soc., 1998, 18, 131–140.

[41] Thijs, I., Luyten, J. and Mullens, Steven, Producing ceramic foams with hollow spheres. J. Am. Ceram. Soc., 2003, 87(1), 170–172.

[42] Mehdi Kazemzadeh Narbat, Fariba Orang, Mehran Solati Hashtjin and Azadeh Goudarzi; “Fabrication of Porous Hydroxyapatite-Gelatin Composite Scaffolds for Bone Tissue Engineering” Iran. Biomed. J. 10 (4): 215-223, 2006.

[43] Xiao Huang ,Xigeng Miao; “Novel Porous Hydroxyapatite Prepared by Combining H2O2 Foaming with PU Sponge and Modified with PLGA and Bioactive Glass” journal of biomaterial application, Volume 00 — 2006.

[44] Vassilis Karageorgiou and DavidKaplan;“Porosity of 3D biomaterial scaffolds and osteogenesis”, Biomaterials 26 (2005) 5474–5491.

[45] I. Sopyan, M. Mel, S.Ramesh, K.A. Khalid; “Porous hydroxyapatite for artificial bone applications” Science and Technology of Advanced Materials 8 (2007) 116–123.

[46] H.R. Ramay, M. Zhang, Biomaterials 24 (2003) 3293.

[47] Ohtsuki C, KokuboT, YamamuroT. “Mechanism of HA formation of CaO-SiO2-P2O5 glasses in simulated body fluid”. J Non- Cryst Solids 1992; 143:84-92.

[48] Guang Yang, Lina Zhanga, Hanqiao Feng “Role of polyethylene glycol in formation and structure of regenerated cellulose microporous membrane” Journal of Membrane Science 161 (1999) 31±40